

AD-781 646

THE EFFECT OF A CASE ON AIRBLAST
MEASUREMENTS. PART I. FRIABLE INERT
CASES

William S. Filler

Naval Ordnance Laboratory
White Oak, Maryland

9 April 1974

DISTRIBUTED BY:



National Technical Information Service
U. S. DEPARTMENT OF COMMERCE
5285 Port Royal Road, Springfield Va. 22151

UNCLASSIFIED

SECURITY CLASSIFICATION OF THIS PAGE (When Data Entered)

REPORT DOCUMENTATION PAGE		READ INSTRUCTIONS BEFORE COMPLETING FORM
1. REPORT NUMBER NOLTR 74-62	2. GOVT ACCESSION NO.	3. RECIPIENT'S CATALOG NUMBER AD-781646
4. TITLE (and Subtitle) The Effect of a Case on Airblast Measurements. Part I: Friable Inert Cases		5. TYPE OF REPORT & PERIOD COVERED Technical Report
7. AUTHOR(s) William S. Filler		8. CONTRACT OR GRANT NUMBER(s)
9. PERFORMING ORGANIZATION NAME AND ADDRESS Naval Ordnance Laboratory Air/Ground Explosions Division Silver Spring, Maryland 20910		10. PROGRAM ELEMENT, PROJECT, TASK AREA & WORK UNIT NUMBERS ORD-332-001/092-1/UF20-354-310
11. CONTROLLING OFFICE NAME AND ADDRESS Naval Ordnance Systems Command Washington, D. C. 20360		12. REPORT DATE 9 April 1974
14. MONITORING AGENCY NAME & ADDRESS (if different from Controlling Office)		13. NUMBER OF PAGES <i>35</i>
		15. SECURITY CLASS. (of this report) Unclassified
		15a. DECLASSIFICATION/DOWNGRADING SCHEDULE
16. DISTRIBUTION STATEMENT (of this Report) Approved for Public Release; Distribution Unlimited		
17. DISTRIBUTION STATEMENT (of the abstract or cover in Block 16, if different from Report)		
18. SUPPLEMENTARY NOTES <i>NAVAL ORDNANCE LABORATORY WESBURN, MD 20910</i>		
19. KEY WORDS (Continue on reverse side if necessary and identify by block number) Cased Explosives; Airblast Effectiveness; Airblast Yield; Mass Effect; Energy Partition; Spherical Shock Wave; Pentolite; Explosives Comparison; Fragmentation (PE62611N); Bombs; Warheads; Case Effects		
20. ABSTRACT (Continue on reverse side if necessary and identify by block number) The effect of casing mass on the airblast from high explosives was examined experimentally by making shock wave pressure-time measurements with piezoelectric gages in the peak pressure range from 80 to 4 psi on spherical pentolite charges encased in ceramic and plastic shells of mass varying in 12 increments from about 2% to 33% of the explosive filling weight. From the lightest to the heaviest case shock peak pressure changed progressively from about		

UNCLASSIFIED

SECURITY CLASSIFICATION OF THIS PAGE (When Data Entered)

5% higher to 5% lower than that for a bare charge (7% in Equivalent Weight terms). The yield reduction is 25% less than that predicted by the Fano formula but in good agreement with Fisher's formula based on steel cased data.

These results support the case-fragment-to-blast energy transfer hypothesis discussed in NOLTR 70-66 and shed light, albeit indirect, on detonation behavior near the surface of a bare charge.

UNCLASSIFIED

SECURITY CLASSIFICATION OF THIS PAGE (When Data Entered)

NOLTR 74-62

9 April 1974

The Effect of a Case on Airblast Measurements. Part I: Friable Inert Cases

In attempting to anticipate the effectiveness of a bomb or warhead, it is important, among other things, to know the effect of the casing on the airblast output of the weapon. Over the last several years the Naval Ordnance Laboratory (NOL) has been engaged in reexamining this problem. In a preceding report, NOLTR 70-66, "A New Approach to Airblast from Cased Explosives," some new insights were developed based on analysis of World War II and subsequent data. In the present report NOL data taken in 1967-68 are presented for charges encased in relatively thin inert frangible materials. The small case mass increments used were intended to explore expected airblast yield enhancement for light cased charges relative to bare charges. Later reports will present data in hand on thicker cases, frangible and ductile, reactive and nonreactive. The work was performed under Task ORD-332-001/092-1/UF20-354-310.

This effort was accomplished with the assistance of many individuals and groups. Among the most important was the work of Phillip Peckham and his team who carried out the firing program. Kitty Cummings and Charles Karmel assisted with the data reduction work. Of special note is the assistance offered by the Non-Magnetic Materials Division Ceramic Laboratory in preparing the casing material for Phase I, in particular George A. Thomas and Roger E. Wilson. Finally, thanks is due Leroy Lovett of the Precision Grinding Shop, whose interest and skill transformed Phase I from a hope to a reality.

Mention of commercial firms or products is for product identification only. No endorsement is intended or implied.

ROBERT WILLIAMSON II
Captain, USN
Commander


J. PETES
By direction

CONTENTS

	Page
INTRODUCTION	1
EXPERIMENTAL METHODS	1
1. Cased Charge Fabrication	1
2. Instrumentation and Field Arrangements	3
3. Data Reduction	4
RESULTS	5
DISCUSSIONS AND CONCLUSIONS	6
REFERENCES	8
APPENDIX A--Positive Impulse Determination Using Thornhill's Modified Friedlander Equation	A-1
APPENDIX B--Raw Data for Peak Pressure and Positive Impulse	B-1

ILLUSTRATIONS

Figure	Title
1.	Materials Representative of Casings Used in Each of the Three Phases
2.	Gage-Charge Field Array
3.	Shock Pressure Histories from 8 lb Pentolite Spheres
4.	Relative Peak Pressure Versus Case Weight Ratio (S/X)
5.	Airblast Equivalent Weight, $\frac{W}{W_0}$, for Cased Relative to Bare Charges Based on Peak Shock Pressure

TABLES

Table	Title
1	Test Charge Specifications
2	Mean Peak Pressure (PSI) - All Phases
3	Relative Peak Pressure (&Change from Bare Charge Values)
4	Positive Impulse - Phase III <ul style="list-style-type: none"> a. Mean Values (psi-msec) b. Relative Values (%)

THE EFFECT OF A CASE ON AIRBLAST MEASUREMENTS.
PART I: FRIABLE INERT CASES

INTRODUCTION

The purpose of this experimental study was to examine the effect of the mass of a case on the airblast yield of a high explosive. Data were derived from shock wave pressure histories obtained with piezoelectric blast gages. A special effort was made to control variables that might make interpretation of results more complex than necessary. In particular, a spherical charge shape was used and only relatively inert substances were employed as case materials. Glass was discarded because of the high cost of securing uniform spherical case thicknesses. Several ceramics* and wall plaster were finally used in the program. The use of frangible materials that become finely subdivided and rapidly decelerate in air had an additional practical consequence for this part of the program--special protection against fragment damage to gages, structures, and personnel was not required.

EXPERIMENTAL METHODS

1. CASED CHARGE FABRICATION. The effort reported here was carried out in three phases (Table 1). The first phase called for the use of cases whose thickness was as small as could be fabricated (in the range of 0.010 inches).

Early consideration of glass as the case material foundered on the difficulty of obtaining thin but uniform thicknesses at reasonable cost. Mass production glass spheres (used for Christmas tree ornaments) are thin and have very good sphericity but vary in thickness by a factor of two or more in a single glass sphere. Grinding glass spheres to shape was prohibitively expensive for this program because of the quantities involved. The limited strength of plaster of paris in thicknesses less than about 0.100 inches precluded the use of that material in the first phase effort. Consultation with commercial ceramic manufacturers indicated that a lower limit of about 0.040 inch thick ceramic hemispheres was the best that such sources could provide. For the type of material involved, these would have weighed about 6% of the explosive filling weight--higher than what was hoped for.

As a result, in-house capability for ceramics fabrication was considered. A flame spray technique was adapted to produce 6.5" inside diameter Al_2O_3 hemispheres that had sufficient strength not only for

* The word ceramic is used loosely here, since, in order to minimize shape distortion, none of the material was heat treated.

handling purposes but also for grinding to a uniform thickness down to 0.010 inches. In this method an aluminum hemispherical mandrel is slowly rotated in front of a hand-held high-temperature spray gun that automatically feeds a solid rod of the raw material into a hot vaporizing flame. It takes about 10 minutes for 0.010 inches of thickness to be deposited and thus was slow, tedious, and impractical for thicknesses much above 0.030 inches. The shells that were produced have as good sphericity as the mandrel but are of irregular O.D. and, therefore, thickness. However, without heat curing (and the almost certain risk of shape distortion) they have adequate strength for machine grinding.

This was done in the NOL precision grinding shop with the shell supported on the same mandrel used for flame spraying. As a result of an unusual special effort, shells were produced with thicknesses of 0.010, 0.020, and 0.030 and a variation of no more than + .001 inches for the greater part of the shell surface. Spheres with these thicknesses weighed 1.8, 3.6, and 5.2% of the explosive filling weight--a very satisfactory gradation for the purposes of this program.

The second phase involved the purchase of shells with thicknesses 0.04, 0.06, 0.08, and 0.10 inches from the Coors Ceramic Corporation. Cost considerations necessitated the use of available materials and tooling. As a result, a different ceramic was used that consisted of equal proportions of Al_2O_3 and SiO_2 with 1% of other ingredients. These shells had a 6 inch I.D. (resulting in an explosive filling weight of about 6 pounds instead of the 3 pounds used in all the other cased charges fired in this program). The method of fabrication involved a curing process that resulted in shells that had greater variation in shape and thickness than the first phase shells but were tolerable for the purposes of these tests. The basic requirement was that variation of individual case weights be no more than 0.004 inches or 20% of the thickness increment of 0.020 inches. For the large majority of shells used this requirement was satisfied.

Because of the difference in material and production method, density for the Coors shells was lower than the NOL ceramic shells. This in turn, fortuitously resulted in the Coors 0.040 inch shell and the NOL 0.030 inch shell having about the same percentage weight of their respective explosive fillings--a useful overlap for comparison purposes. The largest case weight as a percent of explosive filling weight produced by this method was about 14%.

In the final phase, shells of non-fibrous gypsum wall plaster were fabricated at NOL using as the inner form the same 6.5 inch diameter aluminum mandrels employed in fabricating the NOL thin ceramic shells of the first phase. The outer form was a two-piece mahogany wood mold that was machined to progressively larger size after each set of shells of a required thickness was completed. It was necessary to spray an appropriate freeing compound on the wooden mold surface before each casting. Shell thicknesses of 0.100, 0.200, 0.300, 0.400, and 0.500 were produced by this technique. The plaster of paris shells were of lower density than both previously

described materials, and covered a weight range from about 8 to 33% of the explosive filling weight. During manufacture, poor control of the plaster mix resulted in unwanted variations in density and nonuniformity in weight progression from one shell thickness to the next. However, this is of no apparent importance. Figure 1 shows casings typical of those used in each phase of this effort.

Preparation of the charges for field use involved casting the explosive melt directly into the casing hemispheres. After cooling, the hemispheres were paired and bonded with adhesive. For detonator access, a 1/4 inch diameter hole extending from the surface to a point 1/4 inch beyond the center of the charge was cast into the explosive. The bare charges used in the program were cast as monolithic spheres and drilled for detonator access. The high explosive used throughout was Pentolite, 50% TNT and 50% PETN. Its sensitivity is adequate to allow direct initiation with a detonator, in this case an "Engineer's Special".

2. INSTRUMENTATION AND FIELD ARRANGEMENTS. The data of this report were obtained from recordings of the pressure history of the shock wave at various distances from the charge. Means similar to those of references (1a) and (1b) were used to record and analyze the data obtained. Twelve channels of piezoelectric airblast instrumentation were used. The transducers were Atlantic Research LC 33 units with lead zirconate titanate sensing elements, reference (2). These elements are 1/4 inch long and 1/2 inch in diameter mounted coaxial to and at mid-length along a cylinder of high length-to-diameter ratio. This arrangement minimizes the disturbance to the airflow and its pressure at the sensing element.

A signal generated by a gage is processed and displayed on an oscilloscope as a spot deflection. Permanent recording is done on 35mm film strips mounted on rotating drums that provide a relatively long time base. A system response check and amplitude calibration is accomplished by means of an integral square step method, reference (1). A time base calibration signal of one kHz was provided by a square step generator. The timing pulse is coupled into the signal channel and appears superimposed on the signal trace.

The charge and gages were arrayed in a plane 12 feet from the ground in order to avoid ground reflected shocks during the time of interest. Five distances were chosen; 7, 9, 12, 17, and 29 feet to encompass a pressure range from about 4 to 80 psi. For each distance records were obtained from 2 or 3 gages located on as many different radials. Charges were suspended in fishnet material weighing a few grams with the intent of minimizing the amount of combustible extraneous mass in proximity to the charge. Figure 2 shows the field array.

A group of bare pentolite charges was fired with each of the three groups of cased charges. These served as a control on potential unsuspected instrumentation and environmental variables that might affect comparative results mainly within each of the several phases;

they also provided a comparison with the accepted standard airblast output of pentolite. Firing took place over a period of 15 months at the NOL Airblast Facility, Stump Neck, Maryland as follows:

Phase One - 2 October to 17 November 1967
Phase Two - 9 February to 7 March 1968
Phase Three - 11 November to 31 December 1968

3. DATA REDUCTION. Measurements were made on each pressure-time record as traced from a magnified projection of the film. Since at high shock pressures, the natural resonant frequency of the gage sensing element was superposed on the shock decay the resulting trace required interpretation to determine the correct peak amplitude of the shock. Figure 3 illustrates the type of records obtained.

In Phase II, the closest gages produced a very high percentage of records that were grossly abnormal in appearance (Figure 3). Even those in the group that were considered readable in the usual sense gave average values for peak pressure that were inconsistent with the data at all other distances for the phase and with data at the same distance from the other phases.

The reason for the difficulty was not established. Since exchanging gages with other locations did not correct the problem, it was assumed to be associated with processes external to the gage. One possibility might involve aerodynamic interaction of case fragments with the blast wave at the time of gage encounter. The mass and size of fragments resulting from the case material of the second phase may have been such as to maximize irregularity in the blast wave at the time it passed the nearest gages.

Consider two limiting situations. In one, a case becomes so finely pulverized at the time of detonation that it very quickly becomes undifferentiable from the gas of the explosion. Velocity and thermal equilibrium exists between particles and gas when the gages are passed by the blast. The gage will respond to the gas pressure, but the particles go essentially unobserved.

In the other, a case produces fragments large enough to be projected eventually out ahead of the gas expansion (permanently so far as blast measurements are concerned). We might expect gages to first record disturbances from the bow waves of fragments moving through undisturbed air. Eventually the main shock comes along reinforced by energy from the preshocked air (due to the bow wave disturbances having become substantially well distributed).

Now consider a third case that produces fragments intermediate in size compared with the above. These get ahead of the main gas expansion but by the time the first gage is reached the fragments themselves are just being overtaken by the main shock. Their bow shock pressure disturbances, positive and negative, instead of being well ahead are recorded nearly coincidentally with the main shock. Such interactions would be recorded as grossly abnormal pressure histories. This probably is the correct explanation of the anomalous records.

As to why this occurred only in Phase II, one must consider the materials involved. Both the thin material of Phase I and the plaster of paris of Phase III most probably produced powder-like fragments, whereas the ceramic used in Phase II could likely have produced a distribution of fragment sizes large enough to have a substantially different aerodynamic behavior.

Although all readable data are included in this report, data for $R = 7$ feet, Phase II was not included in the final evaluation (see Table 3).

Positive impulse was determined for Phase III as representative of the program since its data overlapped the other results not only in S/X* but in all significant peak pressure trends.

The methods used in this study to determine positive impulse involves the use of the integrated form of a modified Friedlander equation due to Thornhill (Appendix A). The excellent agreement described in reference (3) between recorded pressure-time curves and the equation shape was confirmed by us in a pilot comparison between impulse determined by this method and by the planimeter using Phase III data for one distance.

All raw data are included in Appendix B. These data were processed by computer using a Basic Language program for calculating means and precision indices, and rejecting widely deviant data in accordance with Chauvenet's criteria, reference (4). All means so calculated for peak pressure are collected in Table 2 and for positive impulse in Table 4a. Since Phase II tests were conducted with nominal 6 lb charges and since direct pressure comparisons were to be made with the nominal 8 lb standard bare charge it was necessary to scale up the Phase II pressure means for the cased charges. This was done in accordance with the expression

$$P = P_T \frac{W}{W_T}^{\frac{n}{n}}$$

where n is the slope at each distance as derived from the compiled standard pentolite curve, reference (5), P is peak pressure, W is weight of charge, and subscript T indicates test data.

RESULTS

The method of evaluation was to compare peak pressure and impulse mean values for the cased charges directly with values for the bare charges at the same distances. Table 3 and Table 4b give the comparative data in the form of percent increase or decrease relative to the bare charge data. In order to conveniently observe trends grand means were taken along horizontal and vertical columns.

$$*S/X = \frac{\text{shell weight}}{\text{explosive weight}} \times 100\%$$

Overall, the horizontal grand means show a shift from positive to negative as the case mass increases. For pressure the spread is from a high of +6.5% to a low of -4.9%; for impulse +5.2% to -9.4%. Figure 4 is a plot of all the pressure grand means versus S/X that shows the overall pattern more vividly.

Considering the tabular data in greater detail, Phase I with an S/X limited to about 5% shows grand mean pressure increases averaging nearly 5% relative to bare charge values. Phase II data with a broader S/X ranging to 14% also shows a consistant pressure increase for the grand means. However, Phase II results suggest a decreasing trend. Phase III data with the broadest range for S/X that overlaps the other data are consistant with the trends just noted. Here again low S/X values give increased pressure but as S/X extends beyond 10% to 33% relative pressures drop.

The statistical validity of these results is good in the light of the fact that the average of all sigmas of the mean for peak pressure was $\pm 1.8\%$ and for positive impulse $\pm 3.1\%$.

DISCUSSION AND CONCLUSIONS

In these spherical charge tests with a single explosive, pentolite, surrounded by three different types of finely fragmenting ceramic materials that were considered inert, peak shock pressure and positive impulse decreased only when the shell-to-explosive (S/X) weight ratio exceeded the range 15-20%. Even then the extent of the decrease for S/X = 33%, the maximum covered in these tests, was only about 5% for peak pressure and about 10% for positive impulse. For light shells up to about S/X = 10%, a small increase in blast parameters, on the order of 5%, is revealed unequivocally by a massive amount of data. In an earlier analytic report, reference (6), these results along with other data provide the basis for a new hypothesis regarding the general role of a case as it affects air-blast. In Figure 5 we have superposed the results on a plot from reference (6) of various curves used to correct for case effects. Fano's original equation suggests as much as a 25% lower yield than our data. However, Fisher's semi-empirical adaptation of Fano's method to a wide range of actual bomb data is in excellent agreement with our results for S/X values in the range 20-35%. Earlier data does not exist in the range much below S/X = 20% for which our data shows an increase in yield over bare charge yield.

The results reported here are significant in several other respects.

a. The concept (treated in considerable detail in reference (6)) of fragment kinetic energy transfer to the blast is generally supported by the results. That is, the kinetic energy initially imparted to the case mass ultimately influences the blast. Therefore the initial energy partition between the explosive mass and case mass cannot be the sole basis for estimating the case influence on blast as Fano's treatment suggested.

b. The small but statistically significant enhancement for thin casings tends to support the idea frequently suggested that some blast yield loss may occur due to spalling and consequent detonation failure short of the surface of a bare charge. The relatively small amount of added mass next to the surface as shown by our experiments apparently is enough to increase yield and thus demonstrate that such an effect probably occurs.

c. The correlation of our data for frangible ceramic material with Fisher's curve for steel suggests that at least for this S/X range particle size and shape may not be as important as other parameters.

REFERENCES

- 1a. Tussing, R. B., "A Four Channel Oscilloscope Recording System, NOLTR 65-21, Jul 1965
- 1b. Tussing, R. B., "Accuracy and Calibration Requirements of Oscilloscope Recording Systems." NOLTR 65-77. Aug 1965.
2. Fitzgerald, J. W., "Design Considerations for Pencil Type Air Blast Gages," Atlantic Research Corp, Nov 1955, AD 106 290
3. Thornhill, C. K., "The Shape of a Spherical Blast Wave," ARDE Memo (B) 41/59, Fort Halstead, Kent, U. K., Aug 1959
4. Worthing, A. G., and Geffner, J., "Treatment of Experimental Data," John Wiley, N. Y., 1955
5. Goodman, H. J., "Compiled Free-Air Blast Data on Bare Spherical Pentolite," BRL Rep 1092, Aberdeen Proving Ground, Md., Feb 1960
6. Filler, W. S., "A New Approach to Airblast from Cased Explosives", NOLTR 70-66, Naval Ordnance Laboratory, October 1970
7. Thornhill, C. K., "A Unified Theory of Damage from Minor External Blast", ARDE Report (B) 24/57, September 1957

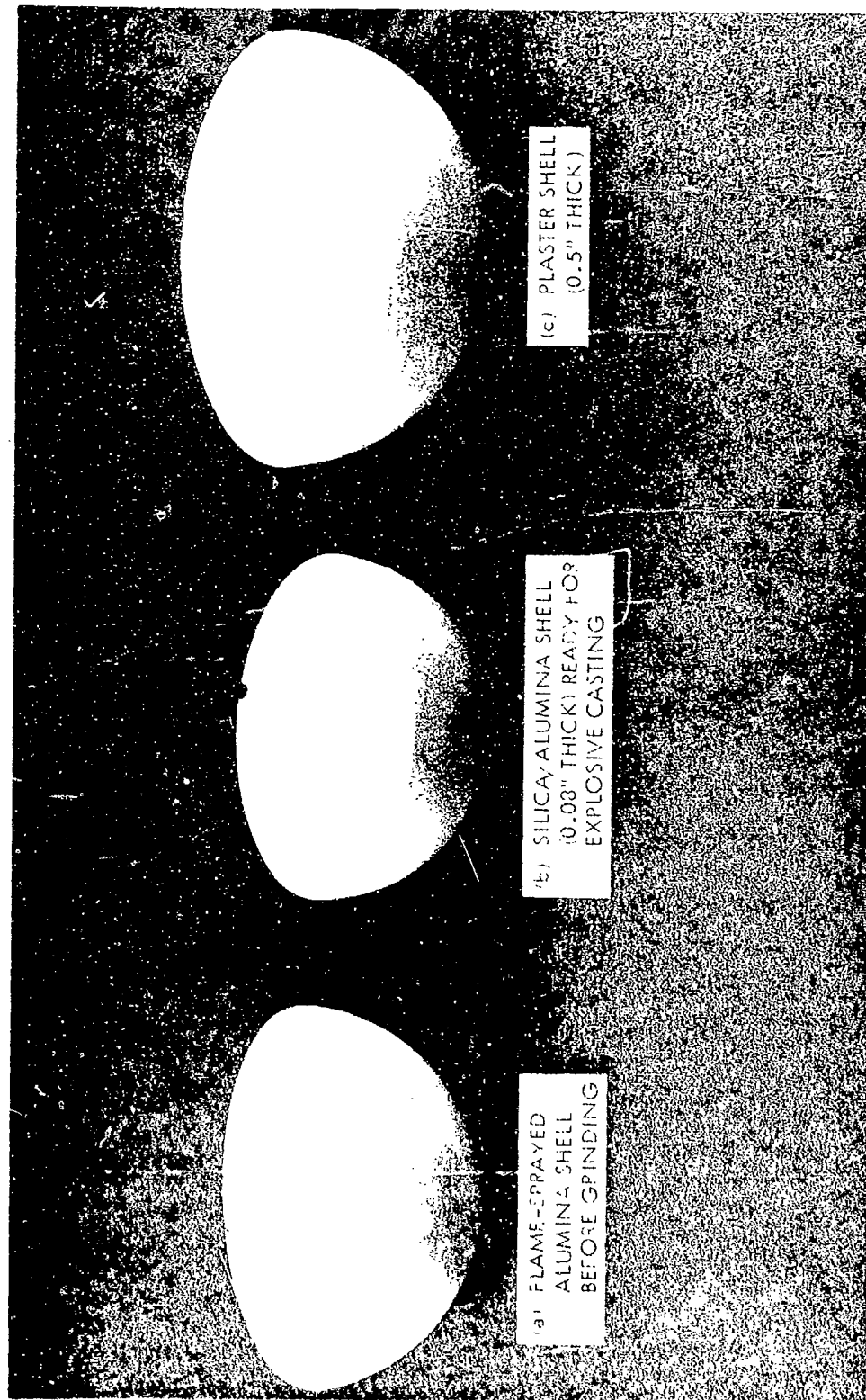
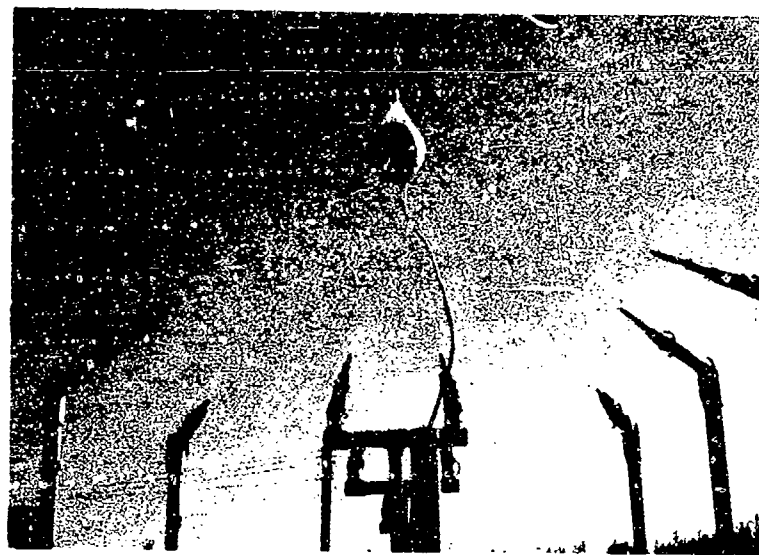


FIG. 1 MATERIALS REPRESENTATIVE OF CASINGS USED IN EACH OF THE THREE PHASES



DISTANCES ARE FROM CENTER OF
CHARGE TO MIDPOINT OF GAGE
SENSOR IN A PLANE 12 FEET FROM
THE GROUND PLANE.

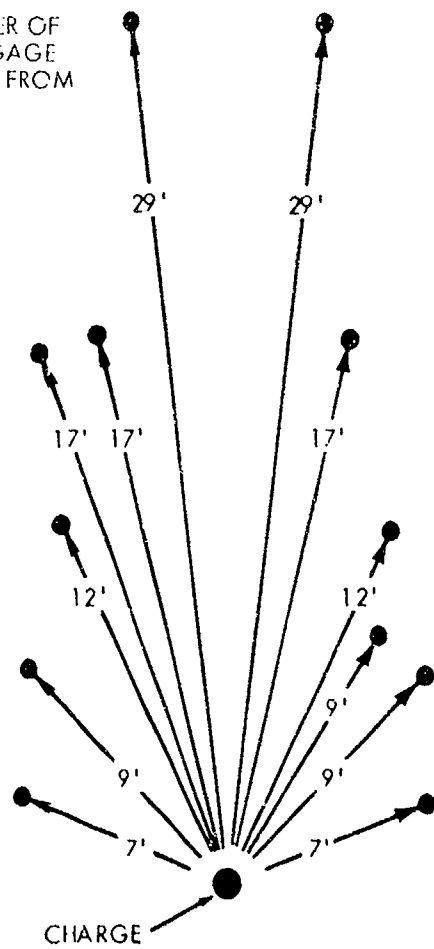
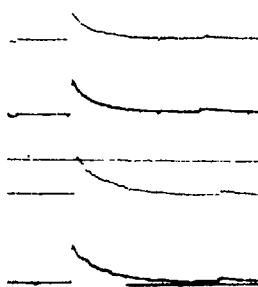


FIG. 2 GAGE-CHARGE FIELD ARRAY

NOLTR 74-62

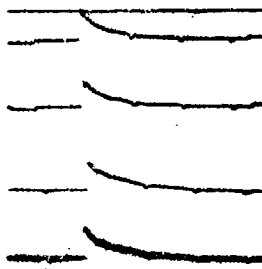
PHASE I

T = 0.03" SHOT 274



PHASE III

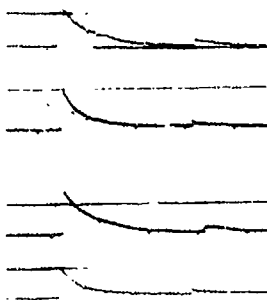
T = 0.40" SHOT 401



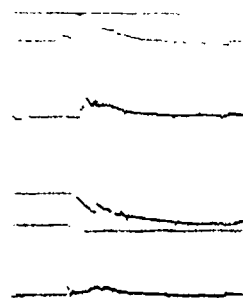
RECORD QUALITY IS GENERALLY GOOD. OCCASIONAL RECORDS
WERE DISTURBED ON OTHER SHOTS.

PHASE II

BARE SHOT 308



T = 0.06" SHOT 307



RECORDS ARE NEARLY SMOOTH
AND "CLASSICAL" IN SHAPE.
INDICATES QUALITY OBTAINABLE.

RECORDS SHOW VARIOUS PERTURBATIONS
SOME WITH PRECURSORS POSSIBLY FROM
FRAGMENT BOW SHOCKS. THESE INDICATE
DEGREE AND VARIETY OF DISTURBANCES.
NOT ALL WERE DISTURBED ON OTHER SHOTS.

FIG. 3 SHOCK PRESSURE HISTORIES FROM 8LB PENTOLITE
SPHERES - PAIRED GAGES AT 7 AND 9 FEET.

NOLTR 74-62

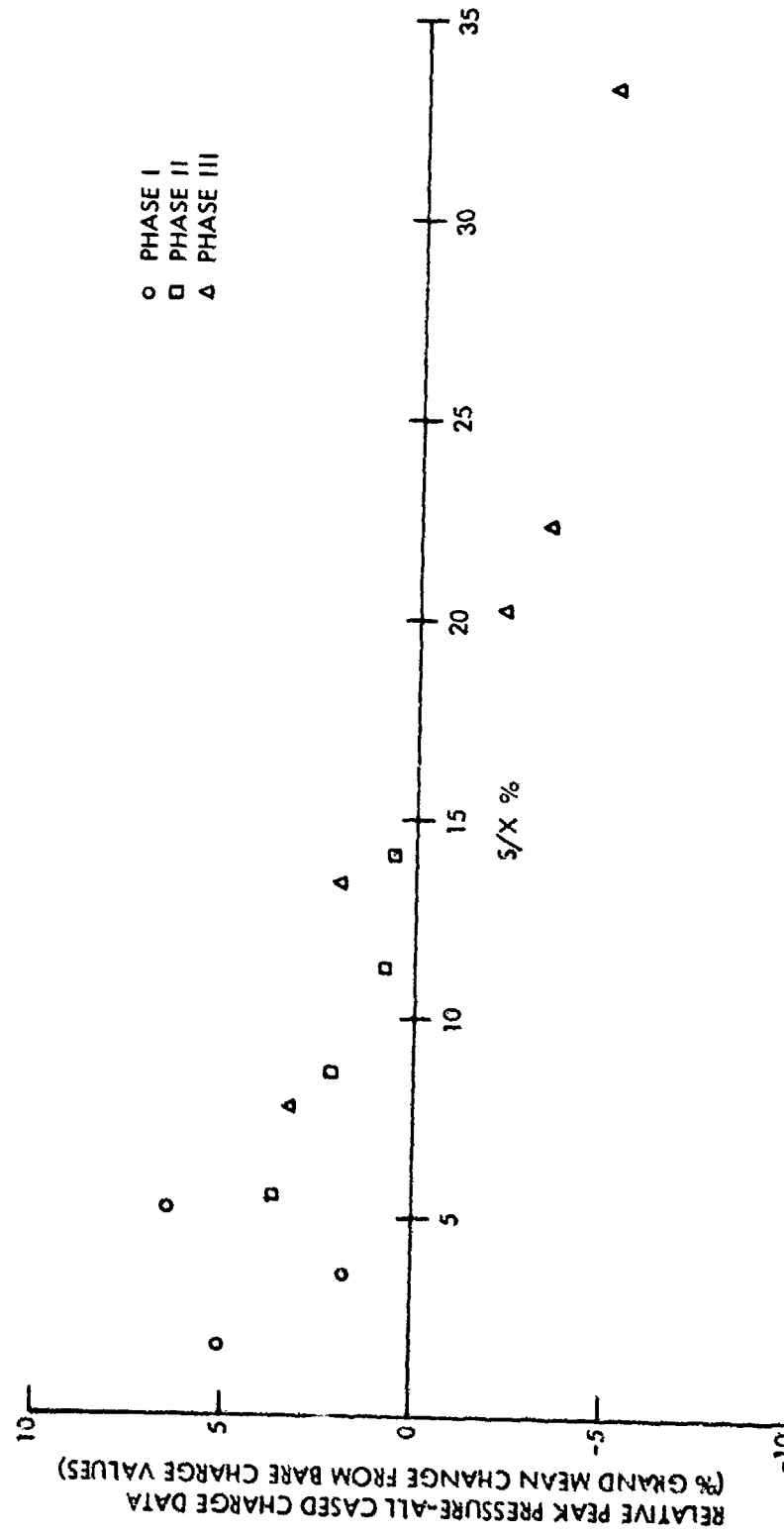


FIG. 4 RELATIVE PEAK PRESSURE VS CASE WEIGHT RATIO (S/X)

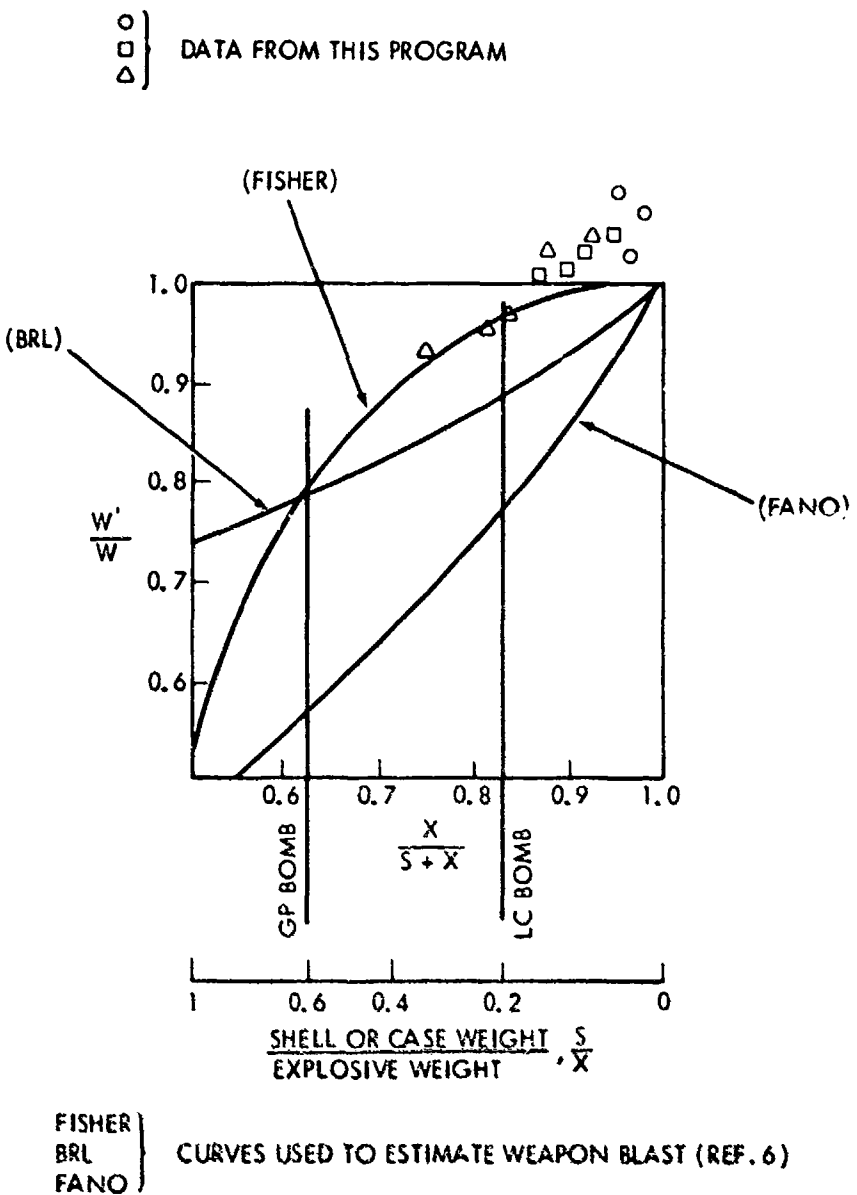


FIG. 5 AIRBLAST EQUIVALENT WEIGHT, W'/W , FOR CASED RELATIVE TO BARE CHARGES BASED ON PEAK SHOCK PRESSURE.

TABLE 1
TEST CHARGE SPECIFICATIONS

Thickness ² T(in)	Material	CASE		Weight S (lb)	Weight X (lb)	EXPLOSIVE ¹	WT RATIO 100 S/X (%)
		Density (g/cm ³)	Weight S (lb)				
PHASE ONE							
0.01	Al ₂ O ₃	3.21	0.150		8.47	8.50 ³	1.8
0.02	"	3.05	0.298		8.36	8.50 ³	3.6
0.03	"	3.23	0.442		8.44	8.50 ³	5.2
PHASE TWO							
0.04	Al ₂ O ₃ /SiO ₂ (50/50)	2.14	0.361		6.42	8.50 ³	5.6
0.06	"	2.18	0.546		6.30	8.50 ³	8.7
0.08	"	2.20	0.706		6.24	8.50 ³	11.3
0.10	"	2.20	0.872		6.13	8.50 ³	14.2
PHASE THREE							
0.1	Plaster of Paris	1.34	0.652		8.39	8.44 ³	7.8
0.2	"	1.18	1.12		8.34	8.44 ³	13.4
0.3	"	1.10	1.71		8.42	8.44 ³	20.3
0.4	"	.89	1.90		8.48	8.44 ³	22.4
0.5	"	1.02	2.81		8.41	8.44 ³	33.4

1. Pentolite: PETN/TNT, 50/50
2. Nominal
3. Bare Charge, Control Standard

TABLE 2
MEAN PEAK PRESSURE (PSI) - ALL PHASES

<u>R(Ft)</u>	<u>7</u>	<u>9</u>	<u>12</u>	<u>17</u>	<u>29</u>
PHASE I					
<u>T(in)</u>					
0.0 (Bare)	77.39	41.28	20.62	9.95	3.92
0.01	85.74	46.19	21.04	9.87	4.03
0.02	79.23	43.46	20.96	10.06	3.87
0.03	84.08	46.12	21.67	10.05	4.17
PHASE II *					
0.0 (Bare)	80.12	42.57	21.41	9.61	3.91
0.04	74.9	46.4	21.0	10.28	3.95
0.06	66.6	43.3	21.0	10.20	4.02
0.08	73.7	41.3	20.8	10.0	4.11
0.1	67.8	43.7	21.2	9.86	3.87
PHASE III					
0.0 (Bare)	76.80	40.36	19.10	9.70	3.92
0.1	79.72	40.75	20.66	9.84	4.00
0.2	79.72	42.56	19.6?	9.76	3.85
0.3	75.18	36.80	19.42	9.74	3.83
0.4	70.82	39.95	18.94	9.72	3.62
0.5	72.42	36.98	19.14	9.47	3.60

*Raw 6 lb charge data (Appendix B) scaled to 8 lb

TABLE 3
RELATIVE PEAK PRESSURE
(% CHANGE FROM BARE CHARGE VALUE)

<u>R(Ft)</u>	<u>1</u>	<u>2</u>	<u>12</u>	<u>17</u>	<u>29</u>	<u>GRAND MEAN</u>	<u>S/X (%)</u>
PHASE I							
<u>T(in)</u>							
0.01	10.8	11.8	2.1	-0.8	2.8	5.3	1.8
0.02	2.3	5.5	1.6	1.1	-1.3	1.8	3.6
0.03	8.7	11.7	5.0	1.0	6.3	6.5	5.2
MEAN	7.3	9.7	2.9	0.4	2.6		
PHASE II							
0.04	-7.8*	9.0	-1.9	6.9	1.0	3.8	5.6
0.06	-18.0*	1.7	-1.9	6.2	2.8	2.2	8.7
0.08	-9.2*	-2.8	-2.8	4.2	5.1	0.9	11.3
0.1	-16.5*	2.7	-1.8	2.6	-1.0	0.5	14.2
MEAN	-12.9	2.6	-2.1	5.0	2.0		
PHASE III							
0.1	3.8	1.0	8.2	1.4	2.0	3.3	7.8
0.2	3.8	5.4	2.7	0.6	-1.8	2.1	13.4
0.3	-2.1	-8.8	1.6	0.4	-2.3	-2.2	20.3
0.4	-7.8	-1.0	-0.8	0.2	-7.7	-3.4	22.4
0.5	-5.8	-8.4	0.2	-2.4	-8.2	-4.9	33.4
MEAN	-1.6	-2.4	2.4	0.0	-3.6		

* Excluded from horizontal means (See Data Reduction)

TABLE 4
POSITIVE IMPULSE - PHASE III

<u>R(Ft)</u>	<u>7</u>	<u>9</u>	<u>12</u>	<u>17</u>	<u>29</u>
--------------	----------	----------	-----------	-----------	-----------

a. MEAN VALUES (PSI-MSEC)

T(In)

0.0 (Bare)	33.68	23.03	16.68	13.14	7.44
0.1	31.56	24.16	17.21	13.07	8.55
0.2	32.75	24.46	18.60	13.51	7.95
0.3	30.20	21.42	18.45	13.38	8.28
0.4	30.42	22.71	15.64	13.35	6.90
0.5	26.84	19.38	16.18	12.40	7.17

b. RELATIVE VALUES (%)

						<u>GRAND MEAN</u>	<u>S/X (%)</u>
0.1	-6.3	4.9	3.2	-0.5	14.9	3.2	7.8
0.2	-2.8	6.2	11.5	2.7	6.8	4.9	13.4
0.3	-10.3	-7.0	10.6	1.7	11.3	1.3	20.3
0.4	-9.6	-1.4	-6.2	1.6	-7.3	-4.6	22.4
0.5	-20.3	-15.9	-3.0	-5.5	-3.6	-9.7	33.4
MEAN	-9.9	-2.6	3.2	0.0	4.4		

APPENDIX A

POSITIVE IMPULSE DETERMINATION USING THORNHILL'S
MODIFIED FRIEDLANDER EQUATION

The Friedlander form for the pressure-time wave shape of a blast wave is

$$\frac{P-P_0}{P-p_0} \approx (1 - \frac{t}{\tau}) e^{-\frac{t}{\tau}} .$$

p = instantaneous pressure

p_0 = ambient pressure

P = Peak pressure

t = instantaneous time

τ = positive duration time

Reference (3) shows the greatly improved accuracy of a modified form of this equation,

$$\frac{P-P_0}{P-p_0} \approx (1 - \frac{t}{2.3\tau_c}) e^{-\frac{t}{2.3\tau_c}} .$$

τ_c = time constant or t at $\frac{P-p_0}{e}$ or $.37\Delta P$

As discussed in reference (3), page 5 and reference (7), page 9, this equation implies that

$$\frac{eI}{P-p_0} \approx 2.3095 \tau_c .$$

I = positive impulse

$\Delta P = (P-p_0)$ peak overpressure

and

$$I \approx 0.85 \Delta P \tau_c .$$

From reference (7), page 9, Equation 3.5, we have $\tau = 2.3095 \tau$. Therefore, we may also calculate the positive phase duration directly from the measured time constant. The time constant itself is readily found with a Gerber adjustable scale. The advantages of this method are that the time, tedium, and error potential of planimeter readings are eliminated, and the effort required becomes comparable to that of a peak pressure determination.

APPENDIX B

RAW DATA FOR PEAK PRESSURE AND POSITIVE IMPULSE

PEAK PRESSURE (PSI) - PHASE I

<u>R(Ft)</u>	<u>7</u>	<u>9</u>	<u>12</u>	<u>17</u>	<u>29</u>
a. BARE CHARGE, CONTROL STANDARD					
<u>SHOT #</u>					
266	73.68	41.83	20.67	10.23	3.77
	73.66	39.94	21.22	9.89	3.95
		39.31		9.66	
268	78.84	41.32	21.93	9.68	3.92
	80.77	43.14	20.91	9.08	4.01
		42.54		10.14	
273	78.58	42.22	18.93	9.64	3.78
	79.89	42.43	19.27	9.44	3.88
				10.55	
275	74.72	40.54	21.73	10.94	4.03
	78.98	40.57	20.32	10.31	4.03
				9.84	
b. T = 0.01 INCHES, S/X = 1.83					
272	83.76	43.50	19.66	9.91	4.03
	85.67	45.34	20.56	10.23	4.00
		41.29		9.80	
276	82.58	45.85	20.33	9.22	3.99
	78.90	49.13	17.70	9.82	4.23*
		51.40		10.63	
280	81.42	50.45	22.77	9.60	4.07
		45.09	23.55	9.49	4.07
		50.04			
281	91.54	45.83	19.70	9.33	3.97
	58.37*	42.26	21.61	9.64	3.99
		46.22		10.26	
284	96.33	46.91	23.11	9.66	4.09
		44.30		10.58	4.05
		45.27		10.00	

* Data rejected by Chauvenet's criteria

APPENDIX B
PEAK PRESSURE (PSI) - PHASE I (Continued)

<u>R(Ft)</u>	<u>7</u>	<u>9</u>	<u>12</u>	<u>17</u>	<u>29</u>
c. T = 0.02 INCHES, S/X = 3.6%					
<u>SHOT #</u>					
269	65.64	42.05	18.24	10.26	3.51
	82.44	41.61	21.16		3.95
		42.05			
270	76.79	37.60	21.76	9.92	
	90.46	41.16	22.51		
		49.30			
277	80.93	58.78*	21.82	9.82	3.98
	77.10	49.63	24.41	9.95	3.87
		44.40		10.58	
278	85.32	36.31	19.53	10.01	4.12
		48.21	22.12	9.80	4.08
282	85.13	43.92	19.47	8.46*	3.76
	109.18*	44.27	18.53	9.67	3.70
		44.42		10.23	
d. T = 0.03 INCHES, S/X = 5.28					
267	81.02	40.56	21.35	9.88	4.48
	79.46	45.88	21.45	9.92	3.97
		41.81		10.13	
274	86.68	43.11	22.08	10.59	4.63
	87.47	43.36		10.73	4.13
		43.35		10.42	
279	85.78	54.52	22.94	9.36	4.24
		59.80	24.94*	10.06	4.15
		50.05		9.77	
283		50.00	20.60	9.68	3.90
		44.99	21.57	10.05	3.87
		46.05		10.02	

* Data rejected by Chauvenet's criteria

APPENDIX B
PEAK PRESSURE (PSI) - PHASE II

<u>R(Ft)</u>	<u>7</u>	<u>9</u>	<u>12</u>	<u>17</u>	<u>29</u>
a. BARE CHARGE, CONTROL STANDARD					
<u>SHOT #</u>					
285		41.08	21.73	10.05	3.96
		43.31	21.68	10.81	3.92
		42.18		9.11	
291	80.20	40.14	20.35	9.45	4.06*
	79.47	42.30	19.31	9.29	3.90
		43.02		8.60	
303	83.82	38.86	24.00	8.82	3.89
	80.86	50.42	15.83*	9.74	3.91
		48.77		9.84	
308	68.00*	38.24	19.67	10.04	3.81
	75.88	44.45	19.91	8.36	3.89
		43.31		10.73	
316	80.46	42.93	24.02	9.29	3.92
		34.19	22.05	10.12	3.97
		45.34		9.95	
b. T = 0.04 INCHES, S/X = 5.6%					
294	74.42*	37.88	15.89	9.36	3.38
	56.28	39.83	14.87	8.41	3.44
297	63.06	35.19	15.50	6.66*	
	59.49			8.25	3.29
				8.30	3.28
311	55.21	33.59	18.72	8.68	
	64.81			7.40	3.52
314	59.71	37.02	17.44	8.26	3.22
	59.98		19.30	8.45	3.81
				8.25	3.69
318	57.30	36.72	18.42	8.36	
	61.55	39.79	10.56*	7.99	3.15
				8.56	
				8.41	4.15*

* Data rejected by Chauvenet's criteria

APPENDIX B
PEAK PRESSURE (PSI) - PHASE II (Cont'd)

<u>R(Ft)</u>	<u>7</u>	<u>9</u>	<u>12</u>	<u>17</u>	<u>29</u>
c. T = 0.06, S/X = 8.7%					
<u>SHOT #</u>					
287	47.52	33.42	16.74	7.42	3.45
289	68.66	38.81 30.96	19.09 17.99 18.39	7.94 8.51 8.68	3.21 3.68 3.62
293	60.49	38.61 37.07	19.00 15.62	7.91 9.40 8.87	3.20 3.18
298			16.42	8.51 8.28	3.38
304	47.00	32.15 31.99	16.68 16.78	8.13 8.46 8.85	3.65 3.50 3.66
307		37.50	15.20 9.90*	7.94 8.02 8.58	3.42 3.57
309	40.04	29.84 37.64	16.71 15.56	8.02 8.85 8.66	3.47 3.32
319	51.93	34.19 30.20	17.88 16.64	7.80 8.26 8.25 9.05	3.50 3.55
d. T = 0.08, S/X = 11.3%					
288	64.37	40.31	19.05	8.68	3.67
290	58.74 56.97	31.71 33.14	15.78	8.47 7.64 7.88	3.54 3.59 3.33
295	63.08	31.54 41.29	14.47	8.20 8.52 8.01	3.41 3.33
299	81.36*	32.49 22.17	15.46	7.35 8.20 8.18	3.23 3.09
	60.04		17.54	7.97	

* Data rejected by Chauvenet's criteria

APPENDIX B
PEAK PRESSURE (PSI) - PHASE II (Cont'd)

<u>R(Ft)</u>	<u>7</u>	<u>9</u>	<u>12</u>	<u>17</u>	<u>29</u>
d. T = 0.08, S/X = 11.3% (Cont'd)					
<u>SHOT #</u>					
300	61.95	27.16	18.54 14.66	7.50 7.31 8.46	3.38 3.15
305	51.72	36.04 29.32	18.92	8.60 8.73 8.48	3.52* 3.87*
312	48.68	35.52		6.38* 9.28 8.89	3.45 3.25
e. T = 0.10, S/X = 14.2%					
286	49.73	33.26 31.49	17.19	8.07 7.80	3.47 3.01
292	49.42	38.37 36.57 39.42	10.74* 18.14	8.48 7.94 7.11	3.33 3.19
296	45.84 55.20	28.77 35.26	15.83 14.70	6.94 7.75	3.58 3.33
301	49.75	31.71 47.97	16.46	6.59 7.81	3.40
302	64.00	32.76 41.55	18.87 18.28	9.08 7.96 9.01	3.17 3.54 3.53
306	56.66	29.76 36.54	17.84 17.01	8.92 8.32 8.25	3.15 3.31
310	61.83 51.06	38.26 34.87	18.27	9.29 7.74	3.39
315	51.26	34.58 28.70	19.93 17.19	8.27 8.32 8.05 8.76	3.44 3.18 3.28

* Data rejected by Chauvenet's criteria

APPENDIX B
PEAK PRESSURE (PSI) - PHASE III

<u>R(Ft)</u>	<u>7</u>	<u>9</u>	<u>12</u>	<u>17</u>	<u>29</u>
--------------	----------	----------	-----------	-----------	-----------

a. BARE CHARGE, CONTROL STANDARD

SHOT #

360	73.4 81.1	42.08 43.31 41.46	21.06 19.06	9.64 9.36 9.48	3.84 3.78
368	79.0	37.50 44.00 38.90	17.27 19.75	10.15 10.05 9.82	3.96 3.95
369	75.1 78.9	39.70 45.50 36.42	19.92 18.81	9.81 9.78 9.56	3.79 3.91
380	77.4* 91.1*	39.93 38.29	19.05 16.94	9.37 9.52 9.71	3.99
387	81.7	40.30 44.10	20.86 20.85	9.76 9.96	3.99 3.95
300	70.4 74.3	39.93 35.70 40.40 38.53	17.95 17.73	9.27 9.72 9.67 9.92	3.99 3.95

b. T = 0.10 INCHES, S/X = 7.8%

362		46.20 42.10 32.04	20.01 19.34	10.06 9.52 10.08	4.03 3.99
365	80.2 81.4	40.80 42.60 45.25	20.86 23.41	10.05 9.67 9.65	3.99 3.95
371	76.8	40.20 50.00 41.90	20.66 23.00	10.20 10.37 10.13	4.12 4.07
374	77.7	43.90 41.50 35.24	18.82 18.87	9.53 9.84 9.83	4.03 3.95
379	76.2 86.0	35.90 35.40 37.90	22.10 19.48	9.72 9.40 9.45	3.99 3.93

* Data rejected by Chauvenet's criteria

APPENDIX B
PEAK PRESSURE (PSI) - PHASE III (Cont'd)

<u>R(Ft)</u>	<u>1</u>	<u>2</u>	<u>12</u>	<u>17</u>	<u>29</u>
	c. T = 0.20 INCHES, S/X = 13.4%				

<u>SHOT #</u>					
363	83.5 79.5	44.40 41.00	19.82* 21.59*	9.96 10.10 10.19	4.31* 4.11
366	81.9	40.60 44.52	19.73 19.72	9.74 9.76 9.63*	3.92 3.88
375	77.9 79.0	44.00 43.23*	19.41 19.69	10.42* 9.80 10.01	3.99 3.91
376	76.5	31.70* 40.14	19.59 19.84	9.60 9.80 9.53	3.63 3.64
382	62.3*		19.41 19.34	9.42 9.68 9.45	3.78 3.78
		35.94*			

d. T = 0.30 INCHES, S/X = 20.3

361	78.4 73.1	36.90 37.40	19.86 18.78	9.64* 10.41*	3.99
367			19.86 19.20	9.99 9.96 9.40	
377	54.5	36.77 35.80	18.42 19.69	9.45 9.76 9.97	3.99
381	76.1	37.95 36.00 39.80* 43.27*	18.68 20.84	9.96 9.59 9.70 9.69	3.59 3.76

* Data rejected by Chauvenet's criteria

APPENDIX B
PEAK PRESSURE (PSI) - PHASE III (Cont'd)

<u>R(Ft)</u>	<u>7</u>	<u>9</u>	<u>12</u>	<u>17</u>	<u>29</u>
e. T = 0.40 INCHES, S/X = 22.4					
<u>SHOT #</u>					
393	67.0	37.20		9.67	3.61
	62.2	44.90		9.71	3.61
395	76.6	40.60	19.01	9.93	
	73.2	42.60	19.48	10.04	3.61
		39.08		10.11	3.75*
401	71.9	38.10	19.67	9.48	
	77.9	40.70	18.31	9.64	3.66
				9.76	3.63
402	80.0	39.90	18.39	9.57	
	56.4		18.31	9.64	3.65
				9.76	3.59
403	62.6	36.50	19.11	9.76	
	79.1		19.26	9.27*	3.84*
				9.10*	3.95*
				8.78*	
f. T = 0.50 INCHES, S/X = 33.4					
396	79.4	39.90	19.25	9.49	3.61
	68.4	38.40	19.29	9.72	3.57
		39.08		9.48	
397		37.00	19.25		
		42.90*	19.15	9.72	3.63
		25.74*			3.57
398	78.1	33.50	19.00	9.42	
		43.10	18.86	9.63	3.63
				9.25	
399	69.9	31.20	19.01	9.45	
			19.29	9.14	3.81*
		35.85		9.28	3.59
400	66.3	31.57		9.45	
		35.80	18.50*	9.68	3.62
		38.40	20.09*	9.45	
				9.42	3.59

* Data rejected by Chauvenet's criteria

APPENDIX B
POSITIVE IMPULSE (PSI-MSEC) - PHASE III

<u>R(Ft)</u>	<u>7</u>	<u>9</u>	<u>12</u>	<u>17</u>	<u>29</u>
a. BARE CHARGE, CONTROL STANDARD					
<u>SHOT #</u>					
360	43.66	23.25	11.64*		6.85
	37.90	20.25	15.39		7.55
		22.91		11.68	
368	30.89	20.40	14.68	14.67	8.25
		23.94	16.79	14.52	7.39
		24.80		13.02	
369	33.19	23.62	16.59*	13.34	7.41
	28.84	25.14	21.58*	14.13	7.98
		25.69		13.41	
380	36.18		16.68	12.74	7.46
	42.59	16.97*	16.27	13.76	
		22.13		11.87	
387	31.25	22.27	17.02	13.52	6.78
		22.49	17.01	13.55	7.72
		25.79		13.40	
390	23.94	21.24	18.31	11.98	7.12
	28.42	20.60	18.08	12.33	7.29
		23.91		12.40	
b. T = 0.10 INCHES, S/X = 7.8%					
362			17.86	12.40	8.59
			18.91	12.94	8.48
365	30.60	25.87		11.57	
	27.68	24.27	17.73	13.66	8.48
		24.26	23.87*	14.39	8.57
371	24.81	24.23		13.53	
		17.09*	21.07*	11.70	8.40
		28.48	17.60	14.10	8.30
		28.50		12.92	
374	40.95	23.51	16.80	13.10	8.75
		21.52	16.04	17.63	8.57
		23.96		15.05	
379	32.39	21.36	17.85	12.39	8.81
	32.90	21.36	14.90	11.59	8.02*
		22.55		12.05	

* Data rejected by Chauvenet's criteria

APPENDIX B

POSITIVE IMPULSE (PSI-MSEC) - PHASE III (Cont'd)

<u>R(Ft)</u>	<u>7</u>	<u>9</u>	<u>12</u>	<u>17</u>	<u>29</u>
	c. T = 0.20 INCHES, S/X = 13.4%				

SHOT #

363		22.64 22.65	19.38 19.27	13.98 13.74 18.86	9.52 9.33
366	34.81	22.43 28.38	20.12 17.60	13.25 13.28 14.74	8.66 7.92
375	34.43 31.57	23.19 29.40	23.10 20.09	13.29 13.33 13.62	6.78 7.97
376	33.82	21.56	18.32 15.17	12.24 11.66*	6.67 6.64
382	29.13	23.88	18.15 14.80	14.58 13.22 13.17	8.35 7.70
		25.97		12.85	

d. T = 0.30 INCHES, S/X = 20.3

361	33.32 24.86	15.69 15.90	19.41 15.96*	12.69 15.05	8.14
367			19.24 18.93	14.43 12.28 13.58	
377	26.41	25.00 21.91	18.01 17.58	13.65 14.94 12.28	
381		22.58 19.28 27.17	18.26 17.71	12.28 13.04 13.19 13.18	8.31 8.39 8.31
		27.06 23.91			

* Data rejected by Chauvenet's criteria

APPENDIX B
POSITIVE IMPULSE (PSI-MSEC) - PHASE III (Cont'd)

<u>R(Ft)</u>	<u>7</u>	<u>9</u>	<u>12</u>	<u>17</u>	<u>29</u>
e. T = 0.40 INCHES, S/X = 22.4					
<u>SHOT #</u>					
393	22.78*	20.55		13.15	6.75
	28.55	20.99		12.38	7.06
395	32.56	25.88	17.78	12.66	
	32.98	24.62	14.90	13.65	6.91
		28.24		15.46	6.96
401	29.95	20.09	17.56	12.09	
	29.14	18.68	14.78	13.92	6.53
402	29.92	22.05	14.85	14.53	5.95
	28.76		15.87	11.79	8.06*
403	30.86	23.27	14.62	13.92	
	30.26		14.73	14.53	7.32
				14.11*	7.34
				10.24*	6.38
				12.39	
				12.31	
f. T = 0.50 INCHES, S/X = 33.4					
396	28.35	19.67	18.00	11.70	7.06
	26.74	17.63	16.40	13.63	7.27
397		27.57*		10.46	
		20.44	18.00		
		23.71	17.91		
		19.69		12.39	6.49
398	27.22	15.66	16.15	11.61	
		22.72	13.63	13.92	6.67
		16.76		11.40	
399	22.58	18.83	16.16	12.45	
		18.78	15.58	11.66	7.42
400	29.31	20.39	15.42	14.20	
		18.28	14.52	12.05	6.56
				13.99	7.01
				12.05	7.41
				12.02	

* Data rejected by Chauvenet's criteria